PHYSICAL REVIEW B VOLUME 26, NUMBER 8 15 OCTOBER 1982

Calculation of neutron cross sections for interband transitions in semiconductors

J. F. Cooke
Solid State Division, Oak Ridge National Laboratory, Oak Ridge, Tennessee 37830

J. A. Blackman
Physics Department, University of Reading, Reading, England
(Received 26 October 1981)

It has been proposed that the introduction of the high-flux high-energy pulsed-neutron sources will allow the study of electronic transitions between valence and conduction bands in semiconductors produced by inelastic scattering of neutrons. A theoretical calculation of the cross sections that would be expected in such an experiment is described. Results are presented for silicon and germanium. In calculating cross sections, which are based on an empirical pseudopotential description of the electronic band structure, it has been important to include both the spin and the orbital part of the magnetic scattering. It is found that, for the values of momentum transfer considered (up to about 10 nm^{-1}), it is the orbital contribution that dominates. It is also shown that the matrix elements for the transitions have an important effect. Cross sections are shown for a range of energy and momentum transfer from which it is concluded that the experiment is likely to be possible, but questions of resolution will be of great importance if useful information about band structure is to be obtained.

I. INTRODUCTION

The introduction of the new high-flux high-energy neutron sources (such as the Spallation Neutron Source at the Rutherford-Appleton Laboratory in England, the Weapons Neutron Research Facility/Proton Storage Ring at Los Alamos, and the Intensed Pulse Neutron Source at Argonne) in the next few years will make it possible to perform experiments that currently cannot be carried out. One experiment that has been proposed is the single-particle excitation of electrons across the band gap in a semiconductor. This is an inelastic scattering experiment in which energy and momentum transfers would be measured but, unlike previous inelastic measurements, the energy transfer would be in the few-eV range. Some considerations about the spectrometry for an experiment of this type has already been made by Allen *et al.*[1]

If such an experiment proves feasible, one would hope that it would be a useful tool in the experimental determination of band structure. Angle-resolved photoemission spectroscopy has proved a very powerful tool in the study of valence-band structure, but as yet there is nothing comparable for conduction-band measurements. Optical excitations also provide a certain amount of information through $\vec{Q}$-conserving transitions. With inelastic neutron scattering, non-$\vec{Q}$-conserving ($\vec{Q}\neq 0$) transitions could also be studied and would, at least in principle, provide much more information.

Neutron scattering is a weak probe of matter, describable within the Born approximation. This affords a significant advantage over most other experimental techniques inasmuch that the experiment gives direct information on the chemistry and physical properties of the sample undistorted by the external probe. The theory of neutron scattering from a degenerate plasma in a magnetic field is reported in Ref. 2 and a short review of the dynamic properties of electrons by neutron scattering appears in Ref. 3.

We have carried out an extensive series of calculations of the total magnetic scattering cross section for electronic excitations in semiconductors in order to aid the assessment of the feasibility of the experiment. The interaction of the neutrons with the electrons is the familiar magnetic one in which the cross section contains the spin and the orbital parts. This case has, to our knowledge, not been examined previously. Earlier work on inelastic cross sections for noninteracting electrons has largely concentrated on the free-electron model[4–6] and tight-binding models of *d*-band transition metals.[7,8]

In Sec. II, we summarize the basic formulas for the cross sections which form the basis for the work. We also include a discussion of the momentum-transfer ($\vec{Q}$) dependence of the cross section at low Q ($=|\vec{Q}|$). This can be obtained trivially and enables us to set the work in context with a comparison with the free-electron and tight-binding cases.

A model band structure had to be chosen for the calculation. The one used was the empirical pseudopotential scheme,[9,10] which is the most efficient computationally. For the homopolar semiconductors this is a three-parameter model. The parametrization gives a reasonable representation of energy dispersion, at least as far as fitting to optical data can determine. Pseudopotential wave functions are a linear combination of plane waves, and orthogonalized core terms need to be included to obtain realistic wave functions. Matrix elements are easy to calculate if we use only the pseudopotential wave functions, but can lead to error due to the neglect of the core part. Section III summarizes the relevant pseudopotential formalism and indicates how we have attempted to assess the importance of the core part.

In Sec. IV the results of the model calculations for silicon and germanium are illustrated. We find that the orbital contribution to the cross section dominates over the spin part for all values of $\vec{Q}$ within the first Brillouin zone. We also find strong indications that core corrections indeed are negligible. In Sec. V we summarize the prospects for the experiment.

II. THEORY

The partial differential magnetic cross section for the scattering of unpolarized neutrons can be written in the form[11]

$$\frac{d^2\sigma}{d\Omega\, dE}=\left[\frac{\gamma e^2}{mc^2}\right]^2\frac{|\vec{k}_f|}{|\vec{k}_i|}\sum_{\alpha\beta}(\delta_{\alpha\beta}-\hat{Q}_\alpha\hat{Q}_\beta)\sum_{\lambda\lambda'}p_\lambda\langle\lambda|D_\alpha(\vec{Q})|\lambda'\rangle\langle\lambda'|D_\beta(\vec{Q})|\lambda\rangle\,\delta(E+E_\lambda-E_{\lambda'})\,, \tag{1}$$

where $\vec{Q}=\vec{k}_f-\vec{k}_i$ is the momentum transfer, in units of $\hbar$, E is the energy transfer, and p_λ is the probability distribution of initial states. The carets denote unit vectors. The electron states are labeled by λ, λ' with corresponding energies $E_\lambda, E_{\lambda'}$. The interaction operator $D(\vec{Q})$ is defined by

$$D(\vec{Q})=\sum_\nu e^{i\vec{Q}\cdot\vec{r}}\left[\vec{s}_\nu-\frac{i}{\hbar|\vec{Q}|}\hat{Q}\times\vec{p}_\nu\right], \tag{2}$$

where $\vec{r}_\nu$, $\vec{s}_\nu$, and $\vec{p}_\nu$ are, respectively, the position, spin, and momentum of the νth electron in the system. The two terms in the definition of $D(\vec{Q})$ result from scattering from the electron spins and orbital moments, respectively.

In the one-electron approximation λ is the label of the Bloch states (i.e., $\lambda\equiv n\vec{k}$, where n is the band index and $\vec{k}$ is the wave vector). Assuming that the system is nonmagnetic so that the spin-up and spin-down bands are equivalent, it is straightforward to show that the total cross section can be written as the sum of spin and orbital parts (no cross terms):

$$\frac{d^2\sigma}{d\Omega\, dE}=\left.\frac{d^2\sigma}{d\Omega\, dE}\right|_{\text{spin}}+\left.\frac{d^2\sigma}{d\Omega\, dE}\right|_{\text{orbital}}. \tag{3}$$

The spin part of the cross section is given by

$$\left.\frac{d^2\sigma}{d\Omega\, dE}\right|_{\text{spin}}=\left[\frac{\gamma e^2}{mc^2}\right]^2\frac{|\vec{k}_f|}{|\vec{k}_i|}\sum_{\substack{nm\\ \vec{k}}}|F^{(S)}_{nm}(\vec{k},\vec{Q})|^2(f_{n\vec{k}}-f_{m\vec{k}+\vec{Q}})\delta(E+E(n\vec{k})-E(m\vec{k}+\vec{Q}))\,. \tag{4}$$

The spin form factor $F^{(S)}$ is

$$F^{(S)}_{nm}(\vec{k},\vec{Q})=\frac{1}{V_0}\int d^3r\, e^{i\vec{Q}\cdot\vec{r}}\bar{\psi}_{n\vec{k}}(\vec{r})\psi_{m\vec{k}+\vec{Q}}(\vec{r})\,, \tag{5}$$

where V_0 is the volume of the unit cell, $\psi_{n\vec{k}}(\vec{r})$ is the Bloch wave function, and $f_{n\vec{k}}$ is the Fermi occupation number. The corresponding orbital contribution is

$$\left.\frac{d^2\sigma}{d\Omega\, dE}\right|_{\text{orbital}} = \left(\frac{\gamma e^2}{mc^2}\right)^2 \frac{|\vec{k}_f|}{|\vec{k}_i|}\frac{1}{2|\vec{Q}|^2}\sum_{\substack{nm\\ \vec{k}}} |F^{(O)}_{nm}(\vec{k},\vec{Q})|^2 (f_{n\vec{k}}-f_{m\vec{k}+\vec{Q}})\delta(E+E(n\vec{k})-E(m\vec{k}+\vec{Q}))\,. \tag{6}$$

The orbital form factor is defined as

$$\vec{F}^{(O)}_{nm}(\vec{k},\vec{Q}) = \frac{1}{V_0}\hat{Q}\times\int d^3r\, e^{i\vec{Q}\cdot\vec{r}}[\bar{\psi}_{n\vec{k}}(\vec{r})\nabla\psi_{m\vec{k}+\vec{Q}}(\vec{r}) - \psi_{m\vec{k}+\vec{Q}}(\vec{r})\nabla\bar{\psi}_{n\vec{k}}(\vec{r})]\,, \tag{7}$$

and the notation $|\vec{\vec{F}}^{(O)}\cdot|^2$ is taken to mean the scalar product $\vec{\vec{F}}^{(O)}\cdot\vec{F}^{(O)}$.

The system under consideration is a semiconductor in which the Fermi energy lies in the band gap and the inelastic scattering is due entirely to interband transitions. Most of the earlier neutron scattering calculations have been on either free electron models or tight-binding d-band transition metals. Generally, the limit of small momentum transfer can be examined analytically. To set this work in the context of earlier calculations, we recall the low-Q results previously obtained and consider the behavior that will occur in that limit for the case of interband transitions.

Let us consider first the form of the cross section at low Q and at zero temperature for a single band free-electron gas. It was shown by Doniach[5] that the spin and orbital parts are proportional to Q^{-1} and Q^{-3}, respectively. In fact, the spin part is exactly proportional to EQ^{-1} for $Q<2k_F$ and $E<(\hbar^2/2m)Q(2k_F-Q)$, where k_F is the Fermi wave number.

This Q^{-1} and Q^{-3} behavior will be true generally for intraband transitions, which can be understood from the following reasoning. The joint density of states $\mathscr{D}$ is of the form

$$\mathscr{D} = \int d^3k\, \delta(E+E_{\vec{k}}-E_{\vec{k}+\vec{Q}})\,. \tag{8}$$

For free electrons,

$$E_{\vec{k}+\vec{Q}}-E_{\vec{k}} = (\hbar^2/2m)(Q^2+2k_zQ)\,,$$

where the direction of $\vec{Q}$ is taken to define the z axis. Substitution of this result into Eq. (8) and changing variables from k_z to k_zQ immediately brings out the Q^{-1} factor in the joint density of states. For intraband transitions we can write

$$E_{\vec{k}+\vec{Q}}-E_{\vec{k}} \simeq \vec{Q}\cdot\vec{\nabla}_{\vec{k}}E_{\vec{k}}\,. \tag{9}$$

Insertion of this result into Eq. (8) and expansion of the argument of the δ function about k_0, the value at which it vanishes, will again demonstrate that Q^{-1} can be brought out as a factor.

Now let us consider the form factors. For a plane wave the spin form factor of Eq. (5) is unity for all Q. For more realistic wave functions, $F^{(S)}$ is unity at $Q=0$ and falls off at increasing Q. For a plane wave the orbital form factor in Eq. (7) is just $2\hat{Q}\times\vec{k}F^{(S)}$. To obtain the cross section, an additional factor $k_\perp^2$ (where $k_\perp$ is the magnitude of the component of $\vec{k}$ perpendicular to $\vec{Q}$) must be inserted into Eq. (8). A factor Q^{-1} from the integration and Q^{-2} from Eq. (6) combine to give the Q^{-3} dependence.

Thus the Q^{-1}- and Q^{-3}-dependent spin and orbital cross sections are characteristic of intraband transitions at small Q. Realistic wave functions will lead to form factors that cause a more rapid falling off for large Q.

We now consider interband transitions. Previously, a factor of Q^{-1} arose in the integration in Eq. (8). This depended on the relation in Eq. (9), which no longer holds for transitions between different bands. Thus the Q^{-1} factor is absent. With regard to the spin form factor in Eq. (5), $F^{(S)}_{nm}\to 0$ as $Q\to 0$ for reasons of orthogonality. By expanding $e^{i\vec{Q}\cdot\vec{r}}$ in powers of Q, it can be seen that $F^{(S)}_{nm}\sim Q$ for small Q, unless forbidden by parity considerations. The spin part of the cross section is thus proportional to Q^2 at small Q for interband transitions. It, of course, falls off in the familiar way for large Q.

The gradient operator in Eq. (7) has nonzero matrix elements even when the factor $e^{i\vec{Q}\cdot\vec{r}}=1$, unless the wave functions possess special symmetry. No dominant Q dependence arises from the orbital form factor and, therefore, the orbital part of the cross section is proportional to Q^{-2} from Eq. (6). We note that four powers of Q distinguish the two components of the cross section, and the orbital part is likely to dominate at the lower values of momentum transfer.

For completeness we also consider the low-Q behavior of the tight-binding d-band calculations[7,8] of nickel. The basis was the five-component $l=2$

manifold. The spin part of the cross section at low Q is dominated by intraband transitions and the Q^{-1} behavior referred to above is valid.

In the tight-binding approach used by Lovesey and Windsor,[8] only d symmetry bands were included, and the overlap between the d ($l=2$) wave functions on different sites was neglected. The gradient operator in Eq. (7) has zero matrix elements between states with the same l value. Thus $F^{(O)}\rightarrow 0$ for $Q\rightarrow 0$ and one can write $F^{(O)}\sim Q$. The Q^2 factor from the form factor cancels the Q^{-2} from Eq. (6). Furthermore, $F^{(O)}$ is only nonzero for transitions between different tight-binding bands. For interband transitions we have shown that no additional Q^{-1} factor appears from the integration of Eq. (8). Thus in the tight-binding model the orbital cross section tends to a constant at low Q, as found by Lovesey and Windsor.[8]

The difference in behavior between the tight-binding model as used by Lovesey and Windsor and the general results obtained above arises from the neglect of overlap of the tight-binding basis functions associated with different sites and from consideration of only the d symmetry terms. While these restrictions may not be too important for calculating other properties of d-band metals, we have demonstrated that they have a dramatic impact on the behavior of the scattering cross section at low Q. Thus it is necessary to exercise some care when approximating wave functions in order that the divergent behavior near $Q=0$ is treated correctly.

III. COMPUTATIONAL DETAILS

To perform the Brillouin-zone sums in Eqs. (4) and (6) in a realistic time, it is necessary to use a band-structure routine that efficiently generates the electronic energies and wave functions at a general point $\vec{k}$. The calculations described here are based on the empirical pseudopotential method discussed by Cohen and Bergstresser.[9]

We consider the homopolar semiconductors silicon and germanium, which are described by a three-parameter pseudopotential,

$$V_p(\vec{r})=\sum_{\vec{G}} V_G \cos\vec{G}\cdot\vec{\tau}\, e^{-i\vec{G}\cdot\vec{r}}\ , \tag{10}$$

where $\vec{\tau}=a_0(\frac{1}{8},\frac{1}{8},\frac{1}{8})$, $G=|\vec{G}|$, and a_0 is the lattice constant. The summation in Eq. (10) is over those reciprocal-lattice vectors of magnitude 3, 8, and 11 (in units of $2\pi/a_0$). The pseudopotential wave function has the form

$$\phi_{n\vec{k}}(\vec{r})=\frac{1}{\sqrt{V_0}}\sum_{\vec{G}} A_{n\vec{k}}(\vec{G})e^{-i(\vec{k}+\vec{G})\cdot\vec{r}}\ . \tag{11}$$

The number of plane waves used in Eq. (11) was restricted to about 20 by adopting a cutoff parameter E_1 such that $|\vec{G}+\vec{k}|^2\leq E_1$. Additional plane waves, restricted in number by a cutoff parameter E_2, were also included approximately by the Löwdin method. For details, see Refs. 9 and 10. The first step in the calculation is the determination of the electronic energies $E(n\vec{k})$ and the plane-wave expansion coefficients $A_{n\vec{k}}(\vec{G})$, which were obtained by solving the model wave equation

$$\left[-\frac{\hbar^2}{2m}\nabla^2+V_p(\vec{r})\right]\phi_{n\vec{k}}(\vec{r})=E(n\vec{k})\phi_{n\vec{k}}(\vec{r})\ . \tag{12}$$

The pseudopotential method was developed to be an efficient scheme for obtaining energy eigenvalues. We recall that the method is a development of the orthogonalized plane-wave formalism in which the electronic wave function is written

$$\psi_{n\vec{k}}(\vec{r})=\phi_{n\vec{k}}(\vec{r})-\sum_{\vec{G}} A_{n\vec{k}}(\vec{G})\sum_j \alpha^j_{\vec{k}}(\vec{G})\sum_l e^{-i(\vec{k}+\vec{G})\cdot\vec{R}_l}\Theta^j(\vec{r}-\vec{R}_l)\ . \tag{13}$$

The sum on l is over both unit cells and sites within the unit cell, and $\Theta^j(\vec{r}-\vec{R}_l)$ is the jth core wave associated with site l. The coefficient $\alpha^j_{\vec{k}}(\vec{G})$ ensures orthogonalization of ψ to the core states and is given by

$$\alpha^j_{\vec{k}}(\vec{G})=\frac{1}{\sqrt{V_0}}\int d^3r\,\bar{\Theta}^j(\vec{r})e^{-i(\vec{k}+\vec{G})\cdot\vec{r}}\ . \tag{14}$$

The core terms in Eq. (13) are incorporated into an energy-dependent pseudopotential, which is approx-

TABLE I. Pseudopotential parameters in Ry as defined in Eq. (10) for silicon and germanium. Only nonzero terms correspond to $G=3$, 8, and 11 (in units of $2\pi/a_0$).

V_G	Si	Ge
V_3	−0.21	−0.23
V_8	0.04	0.01
V_{11}	0.08	0.06

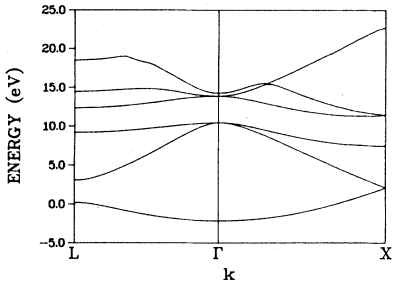

FIG. 1. Energy bands for silicon generated by pseudopotential parameters given in Table I.

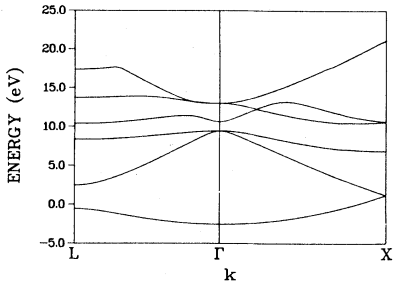

FIG. 3. Energy bands for germanium generated by pseudopotential parameters given in Table I.

imated in the present scheme by $V_p(\vec{r})$ in Eq. (12). The pseudopotential wave functions ϕ should be corrected by the inclusion of core states according to Eq. (13) in order to obtain the true wave function ψ.

If it can be shown that the core corrections have a negligible effect on the scattering cross section, then a considerable simplification in the analysis can be achieved by using the pseudopotential wave functions ϕ alone. The form factors from Eqs. (5) and (7) can then be written in the relatively simple form,

$$F_{nm}^{(S)}(\vec{k},\vec{Q})=\sum_{\vec{G}} A_{n\vec{k}}(\vec{G})A_{m\vec{k}+\vec{Q}}(\vec{G}) , \tag{15}$$

$$F_{nm}^{(O)}(\vec{k},\vec{Q})=-2i\hat{Q}\times\sum_{\vec{G}}(\vec{k}+\vec{G})A_{nk}(\vec{G}) \times A_{m\vec{k}+\vec{Q}}(\vec{G}) . \tag{16}$$

We have attempted to assess the importance of core corrections, which will be discussed at the end of this section. The conclusion is that although they may modify considerably individual matrix elements, the effect on the cross section itself is negligible. Use of Eqs. (15) and (16) can thus be justified.

The numerical evaluation of the neutron scattering cross section was carried out in two steps. First the pseudopotential band-structure equations were numerically solved to obtain the energies and expansion coefficients for silicon and germanium on a regular mesh of about 2000 points in the irreducible Brillouin zone for a face-centered-cubic (fcc) lattice (with two atoms per unit cell). The pseudopotential parameters used in these calculations are given in Table I. We have chosen the coordinate system so that the atoms are located at $\vec{R}\pm a_0(\frac{1}{8},\frac{1}{8},\frac{1}{8})$, where $\vec{R}$ is an fcc lattice vector, which ensures that the $A_{n\vec{k}}(\vec{G})$ are real. The Brillouin-zone sums were evaluated using the tetrahedron method,[12] with 1536 tetrahedra in the irreducible zone. Part of the band structure derived from the parameters in Table I, together with the corresponding density of states, is given in Figs. 1 and 2, respectively, for silicon and Figs. 3 and 4 for germanium.

We consider now the justification for neglecting core terms in the wave function. Some attempts[13,14] have been made to discuss this matter with respect to analogous calculations of the wave-vector-dependent dielectric function. The indications in that work were that the core functions had an insig-

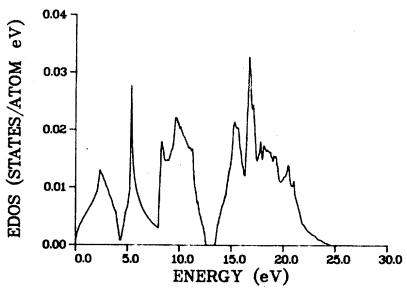

FIG. 2. Electronic density of states for silicon for four valence and four conduction bands.

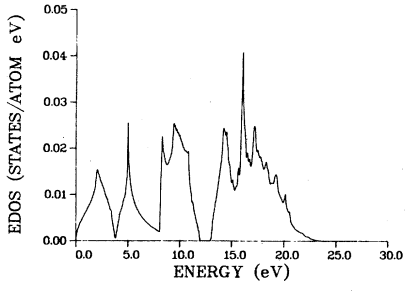

FIG. 4. Electronic density of states for germanium for four valence and four conduction bands.

nificant effect on the dielectric function itself.

To test the effect of core corrections in this case we employed the analytic forms of the core functions ($1s,2s,2p$) given by Woodruff.[15] The overlap coefficients $\alpha^{i}_{\vec{k}}(\vec{G})$ from Eq. (14) can be calculated analytically and included in Eq. (13) to give an approximation to the true wave function ψ. Normalization of the $\psi_{n\vec{k}}(\vec{r})$ was then performed. States of different $n\vec{k}$ are not exactly orthogonal, but this is not important for these purposes.

The modification to the spin form factor in Eq. (15) can also be calculated relatively easily. We were thus able to compare the spin part of the cross section calculated both with and without core corrections. It was found that for a representative momentum transfer,

$$\vec{Q}=\frac{2\pi}{a_0}(0.8125,0,0)\ ,$$

and for all energy transfers up to $E\sim 10$ eV, the difference between the two values is less than 1%. The corrections to the orbital form factor are much harder to obtain. There is no obvious reason to expect that core corrections will be significantly more important for the orbital than for the spin cross sections. Therefore, for this first-generation calculation, the spin and orbital form factors are calculated using only the pseudopotential wave functions.

IV. NUMERICAL RESULTS

In this section we present some of the results from an extensive series of numerical calculations for silicon and germanium. Results have been obtained for $\vec{Q}$ along [100], [111], and [110], and restricted to the first Brillouin zone. The calculations incorporate the full band structure for the four valence and four conduction bands, with higher energy bands being neglected. This should ensure that we obtain the total scattering for energies on the order of 10 eV or less, which is sufficient for our needs. It should be emphasized that one of the main purposes of these calculations is to obtain the magnitude of the cross sections in absolute units (mb/sr eV). All factors in Eq. (1) have been included therefore, apart from the ratio $|\vec{k}_f|/|\vec{k}_i|$, which was set equal to unity. Results for any particular experimental configuration can be obtained by simply multiplying our cross sections by the relevant ratio $|\vec{k}_f|/|\vec{k}_i|$.

In order to investigate the importance of the band and wave-vector dependence of the spin and orbital form factors given in Eqs. (15) and (16) we have also evaluated the joint density of states (JDOS) defined in Eq. (8). A comparison of the JDOS with the total scattering cross section is given in Fig. 5 for silicon with $\vec{Q}=(0.4375,0.0,0.0)$. The JDOS result has been scaled to give the same maximum as the total scattering cross section. This result is typical of the calculations for both silicon and germanium carried out along the three principle symmetry directions in that it establishes beyond any doubt that the band and wave-vector dependence of the spin and orbital form factor cannot be ignored.

A comparison of the spin and orbital scattering cross sections for $\vec{Q}=(0.4375,0.0,0.0)$ is shown in Fig. 6 for silicon and Fig. 7 for germanium. Notice that there is a considerable amount of structure in both components of the scattering and the orbital part is significantly larger than the spin part. The dominance of the orbital part occurred at all values of $\vec{Q}$ we examined, but was less for large $\vec{Q}$. Another important feature of these results is that there is not a dramatic rise in the scattering intensity for E near the indirect gap energy (which in the present pseudopotential parametrization is about 0.9 eV for silicon and 0.8 eV for germanium) as one might expect, at least for appropriate values of $\vec{Q}$. This is due primarily to the same type of behavior that occurs in the JDOS for transitions across the gap, as can be seen in Fig. 5. It is clear, therefore, that no direct information about the band gap can be determined from inelastic neutron scattering experiments.

In order to demonstrate that these observations are quite general, we show a series of plots of the total scattering cross section (with the orbital contribution) as a function of energy for various values of $\vec{Q}$ along the principle symmetry directions in the crystal. Figures 8 and 9 show results for silicon and germanium, respectively. These results also indicate that the cross sections have sufficient structure

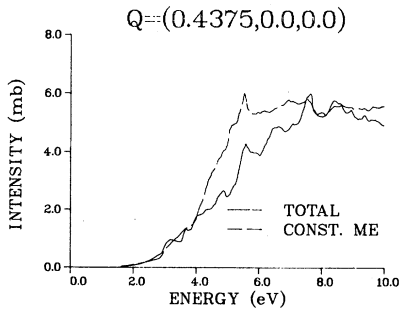

FIG. 5. Comparison of joint density of states vs total scattering intensity for silicon for $\vec{Q}=(0.4375,0.0,0.0)$. Differences are due to matrix element effects.

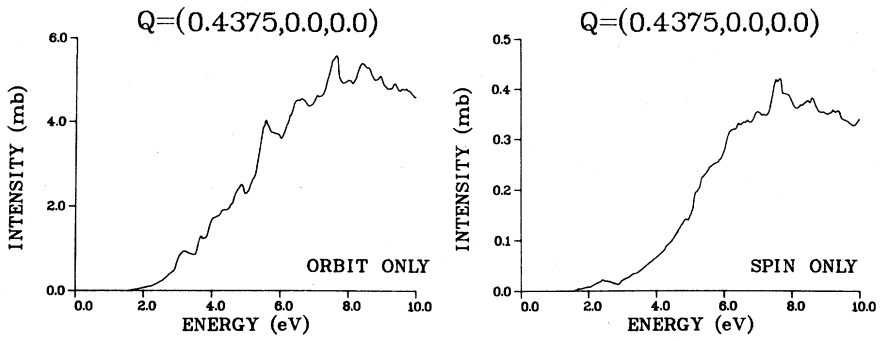

FIG. 6. Comparison of spin and orbital scattering cross sections for silicon. Notice difference in scales.

and variation with $\vec{Q}$ that the band structure, and thus the wave-vector-dependent band gap could, in principle, be determined indirectly. This could be accomplished by varying the pseudopotential parameters to provide the best overall agreement between theory and experiment. This procedure could also provide an indirect check on the validity of the pseudopotential theory. If a good overall fit to the experimental data could not be obtained then we must rely on first-principles methods to generate the band structure. This would not cause any severe numerical difficulties but it would be more difficult to iterate to the "best" one-electron potential.

Finally, we show in Fig. 10 a breakdown of the total scattering for germanium into its individual band-to-band contributions. The contributions shown are from the top two valence bands (labeled $V3$ and $V4$) to the lowest two conduction bands (labeled $C1$ and $C2$). The remaining contributions, which involve $C3$, $C4$, $V1$, and $V2$ (in an obvious notation), do not appear on the diagram. These results indicate that the total scattering cross section is a rather complicated combination of the interband contributions and that the structure found in the cross section cannot necessarily be directly related to features of particular interband transitions.

V. CONCLUSIONS

We will attempt here to indicate the considerations that should be made in assessing the instrumental requirements necessary if neutron scattering is to be a useful technique for band-structure determination. One starts with a band-structure model, ideally with a small number of parameters like the empirical pseudopotential scheme, and assumes that its consistency with the valence band can be determined by angle-resolved photoemission experiments. Optical measurements will then serve to

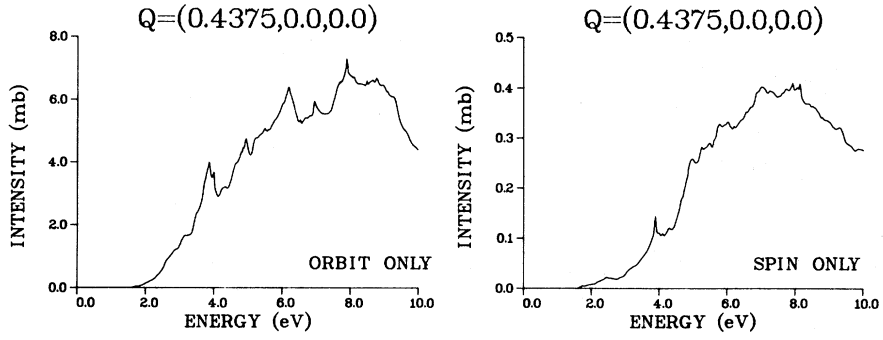

FIG. 7. Comparison of spin and orbital scattering cross sections for germanium. Notice difference in scales.

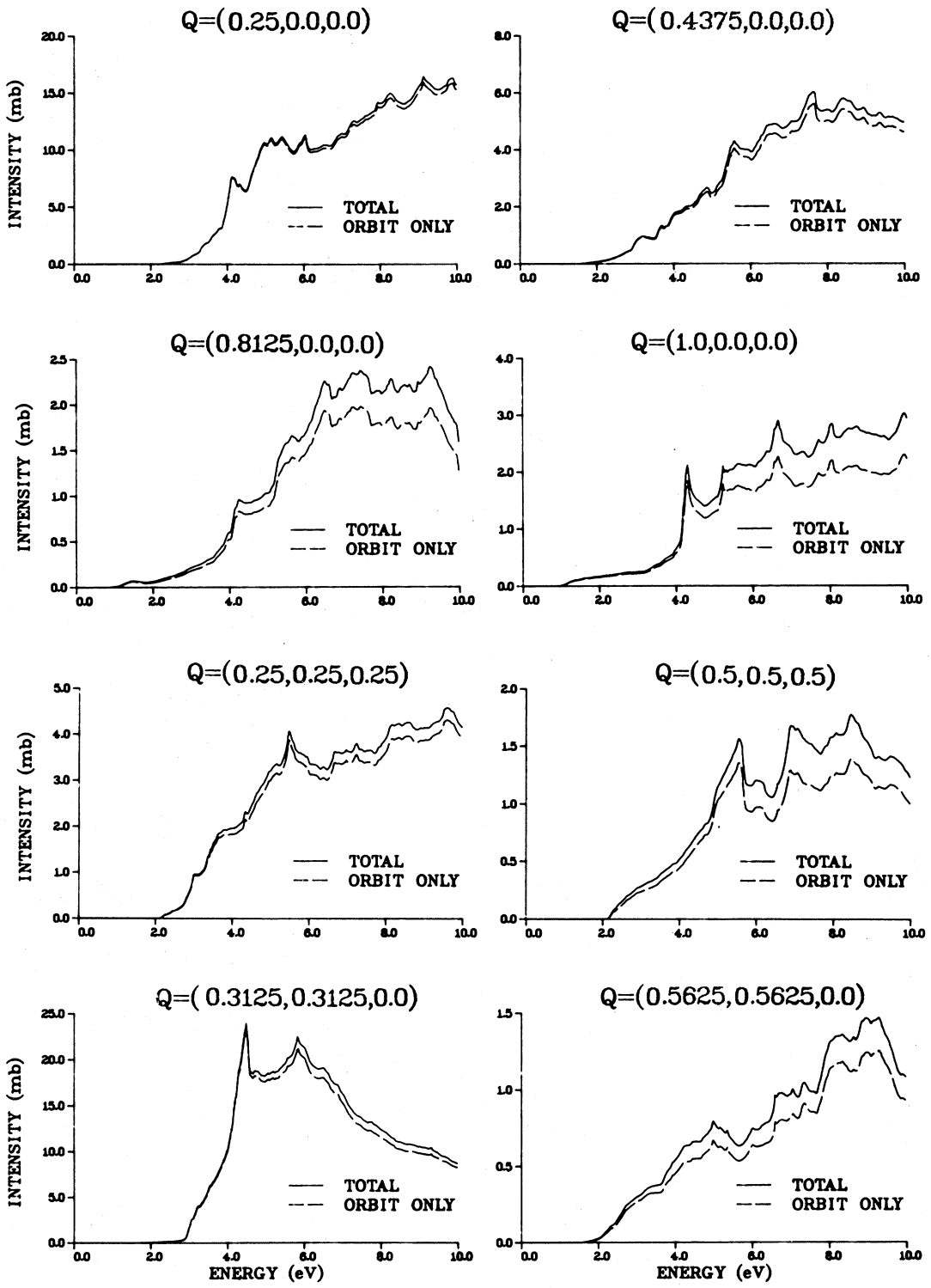

FIG. 8. Results for total scattering intensity and orbital contributions for silicon for several values of $\vec{Q}$ along [100], [110], and [111].

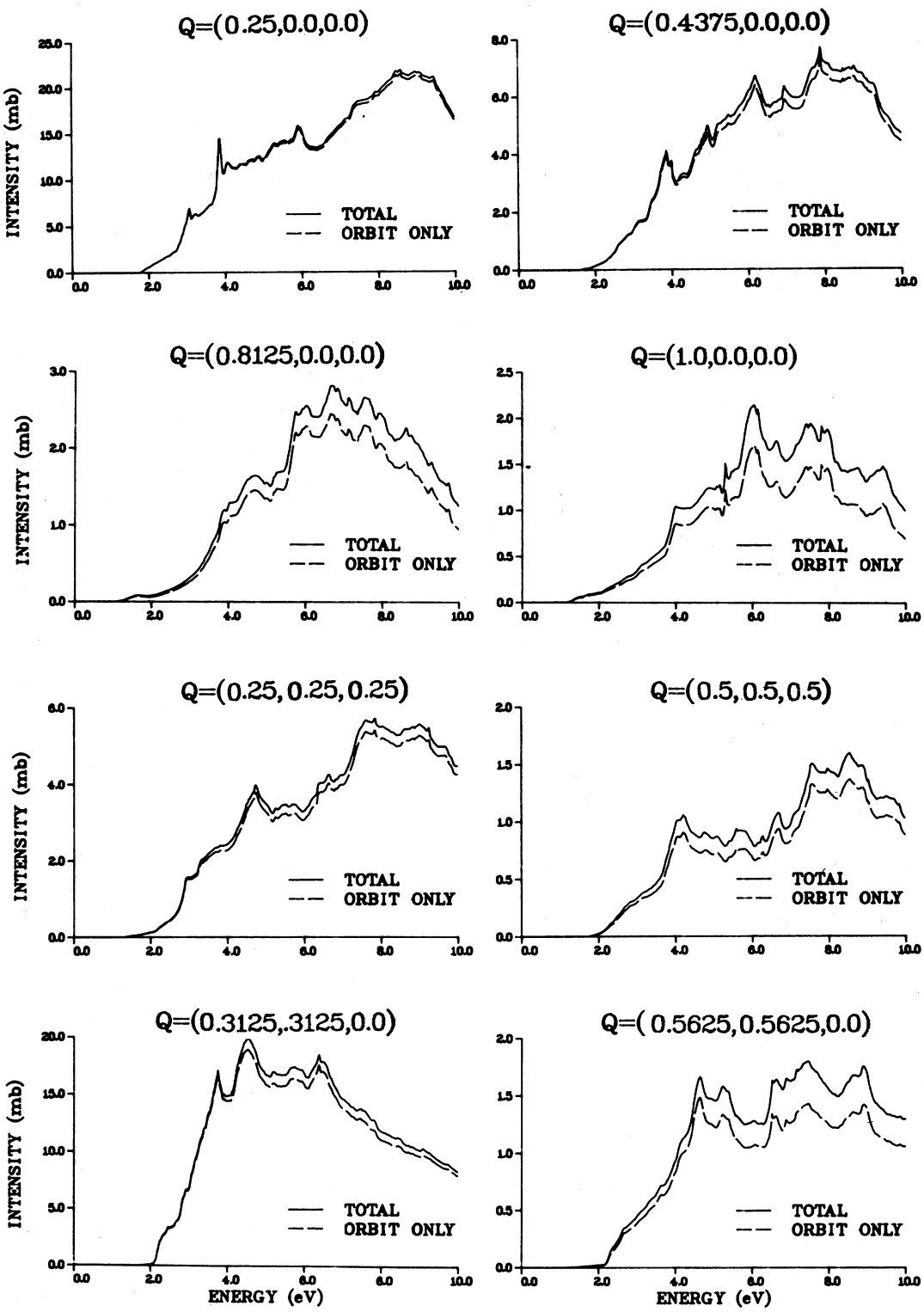

FIG. 9. Results for total scattering intensity and orbital contribution for germanium for several values of $\vec{Q}$ along [100], [110], and [111].

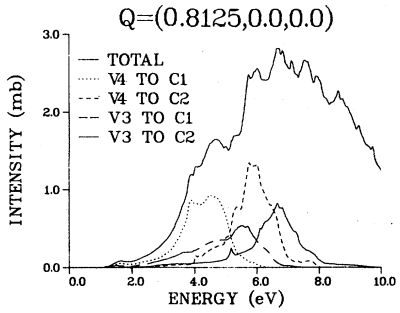

FIG. 10. Breakdown of total scattering intensity for germanium into its individual band-to-band components. $V3$ and $V4$ correspond to the top two valence bands respectively; $C1$ and $C2$ refer to the two lowest energy conduction bands, respectively.

specify a few points in the conduction band. Can neutron scattering complete the test of the consistency of the model with the actual band structure? The answer to this question depends on both intensity and resolution.

The largest value of momentum transfer used in this work was $\vec{Q}=(2\pi/a_0)$ (1,0,0). This is roughly 10 nm^{-1}. The scattering intensity can be estimated by assuming a variation approximately like Q^{-2}. Thus at 20 and 30 nm^{-1} the intensities will be roughly in the ranges 0.25—0.5 and 0.1—0.2 mb/(sr eV), respectively.

We note that although the band gaps in Si and Ge are of the order of 1 eV, the intensity remains negligible until the energy transfer is about 3 eV. To obtain a significant amount of useful information it would be desirable to be able to measure cross sections up to values of E of 7 or 8 eV. As a working hypothesis, therefore, one needs to study energy transfers from about 3 to 8 times the band gap. For the III-V compounds with smaller band gaps, none of the figures so far quoted are outside the range of feasibility considered by Allen *et al.*[1]

Let us now point to some aspects of the figures that will indicate the sort of instrumental resolution required. One first looks for structure. There is plenty of it, but a lot is certainly beyond the limits of resolution. Some of the best defined peaks (at lower energy transfers) in the calculations reported here are near 5 eV for

$$\vec{Q}=\frac{2\pi}{a_0}(1,0,0)\ ,$$

$$\vec{Q}=\frac{2\pi}{a_0}(0.5,0.5,0.5)\ ,$$

and

$$\vec{Q}=\frac{2\pi}{a_0}(0.3125,0.3125,0.0)\ .$$

The band structure of Si and Ge are similar, as can be seen from Figs. 1 and 3. This similarity is reflected in the cross sections. It is instructive to ask which cross sections most clearly distinguish between the two cases. One obvious candidate is the cross section for

$$\vec{Q}=\frac{2\pi}{a_0}(0.5625,0.5625,0)\ .$$

For Ge the intensity increases rapidly for E up to 4 eV, remains roughly constant to about 7 eV, and then increases again. For Si, the intensity increases by about a factor of 2 over the 4—7 eV range of energy transfer, with two narrow plateaus (<1 eV in width) that may be seen as shoulders with reasonable resolution. Clearly, in planning an experiment one must plan to be able to resolve differences such as those just illustrated.

The problem of determining band-structure parameters precisely is similar to that of distinguishing between the cross section for the two similar band structures of Si and Ge. A set of model calculations will indicate the regions of energy and momentum transfer that can be optimally studied. The set of plots displayed in Figs. 7 and 8 should help in the assessment of the resolution on E and Q necessary to make the proposed experiments useful.

From the theoretical point of view, one will need to extend the calculations of the cross sections to larger values of $\vec{Q}$ and to values of $\vec{Q}$ away from the symmetry directions. One also has to bear in mind the approximations made in calculating matrix elements. Hopefully the pseudopotential wave functions will be sufficient. The importance of the matrix elements in the calculation of the cross sections was illustrated in Fig. 5. Clearly in any disagreement with experiment the question of the matrix elements would have to be considered again. It appears from the results we have obtained that the experiment proposed by Allen *et al.*[1] is going to be a difficult one to perform. The successful measurement of these relatively small cross sections would, however, provide important information about the conduction bands in semiconductors that cannot, at present, be obtained from any other source.

ACKNOWLEDGMENTS

This research was sponsored by the Division of Materials Sciences, U. S. Department of Energy under Contract No. W-7405-eng-26 with Union Carbide Corporation. One of us (J. A. B.) is pleased to acknowledge the hospitality of the Solid State Division of ORNL while this work was performed.

[1]D. R. Allen, E. W. J. Mitchell, and R. N. Sinclair, J. Phys. E 13, 639 (1980).
[2]S. W. Lovesey, Z. Phys. B 32, 189 (1979).
[3]S. W. Lovesey, Comments Solid State Phys. 10, 45 (1981).
[4]R. J. Elliott, Proc. R. Soc. London Ser. A 235, 289 (1956).
[5]S. Doniach, Proc. Phys. Soc. London 91, 86 (1967).
[6]J. E. Hebborn and N. H. March, Adv. Phys. 19, 175 (1970).
[7]R. D. Lowde and C. G. Windsor, Adv. Phys. 19, 813 (1970).
[8]S. W. Lovesey and C. G. Windsor, Phys. Rev. B 4, 3048 (1971).
[9]M. L. Cohen and T. K. Bergstresser, Phys. Rev. 141, 789 (1966).
[10]D. Brust, Phys. Rev. 134, A1337 (1964).
[11]W. Marshall and S. W. Lovesey, *Theory of Thermal Neutron Scattering* (Oxford University Press, New York, 1971).
[12]G. Lehmann and M. Taut, Phys. Status Solidi 54, 469 (1972); J. F. Cooke, J. W. Lynn, and H. L. Davis, Phys. Rev. B 21, 4118 (1980).
[13]J. P. Van Dyke, Phys. Rev. B 5, 1489 (1972).
[14]H. Nara, J. Phys. Soc. Jpn. 20, 778 (1965).
[15]T. O. Woodruff, Phys. Rev. 103, 1159 (1956).